JOURNAL OF HEAVY METAL RESEARCH

https://jhmr.hsu.ac.ir E-ISSN: 3116-0522 Journal of Heavy Metal Research, 2026, vol 1, Issue 2, 54-59

Original Article

Enhancing the Activity and Durability of Pt Catalysts through Ceramic Supports in Polymer Electrolyte Fuel Cells

Zahra Anvari Shami[1], Mehrdad Oroji[1]*, Neda Shekarchian[1]

1. Central Laboratory, Pasargad Kavosh Mining Cooperation, Tehran, Iran

* Correspondence: mehrdadoroji@grr.la

Received: 15 June 2026
Revised: 20 July 2026
Accepted: 23 July 2026
Published: 27 July 2026

Publisher: Hakim Sabzevari University

Citation: Anvari Shami, Z. Oroji, M & Shekarchian, N. (2026). Enhancing the Activity and Durability of Pt Catalysts through Ceramic Supports in Polymer Electrolyte Fuel Cells. *Journal of Heavy Metal Research, 1*(2), 54–59.

Abstract

Ceramic-supported Pt catalysts are promising for durable polymer electrolyte fuel cells, where conventional carbon support corrosion remains a major limitation. In this study, SnO_2-supported Pt catalysts were systematically investigated using hard X-ray photoelectron spectroscopy (HAX-PES), X-ray absorption spectroscopy (XAS/EXAFS), and synchrotron infrared (IR) spectroscopy to clarify the interfacial electronic state, local structure, and surface functional groups. The spectroscopic results provide direct evidence for electron donation from Pt to SnO_2 and PtSn alloy formation at the catalyst–support interface, with these electronic modifications becoming more pronounced at higher Pt loadings. Synchrotron IR measurements did not clearly resolve hydroxyl or other surface functional groups on Pt/Nb-SnO_2 under the current conditions, indicating that their direct contribution to catalytic behavior is likely limited, although weak signals cannot be excluded. These findings elucidate the interfacial evolution of Pt/Nb-SnO_2 systems and highlight the critical role of metal–support interactions in tuning the properties of ceramic-supported Pt catalysts, providing essential design guidelines for developing stable, carbon-free electrocatalysts for next-generation fuel cells.

Keywords: Polymer electrolyte fuel cell, Ceramic-supported platinum catalyst, Tin oxide, Catalyst–support interaction, Oxygen reduction reaction

1. Introduction

To achieve carbon neutrality, efforts are underway worldwide to establish a hydrogen-based energy cycle as a sustainable energy infrastructure. Polymer electrolyte fuel cells (PEFCs), which generate electricity from hydrogen, are regarded as a key technology in this context. Further improvements in efficiency and durability are still required for stationary and passenger-vehicle PEFC systems that have already been commercialized. In parallel with the development of hydrogen infrastructure, research and development are also being pursued to expand PEFC applications to commercial vehicles, including heavy-duty trucks, as well as railway vehicles, ships, construction machinery, and other sectors.

For both stationary and transportation applications, high-temperature operation is attractive because it can simplify water management and improve tolerance to impurities; however, it also intensifies degradation of conventional carbon supports. Carbon corrosion accelerates under such conditions, limiting the durability of Pt nanoparticle catalysts supported on carbon. Accordingly, there is strong interest in alternative support materials that can withstand acidic and high-temperature

environments. Ceramic materials such as SnO_2 and TiO_2 exhibit excellent chemical stability under these conditions, and the development of Pt catalysts supported on such ceramics has therefore been actively pursued [Ozouf et al., 2018; Fabbri et al., 2014a; Fabbri et al., 2014b; Yin et al., 2014].

The use of ceramic supports, however, influences catalyst performance in complex ways. Depending on the support properties and interfacial structure, catalyst activity may be improved or suppressed. Important factors include the electronic conductivity at the support–catalyst interface, the electronic state of Pt modified by catalyst–support interactions, and mass-transport effects associated with the support surface. When a semiconducting ceramic support replaces conductive carbon, a Schottky barrier may form at the interface with Pt particles, increasing electronic resistance and potentially lowering fuel-cell performance. On the other hand, some ceramic-supported Pt catalysts exhibit not only superior durability but also higher oxygen reduction reaction (ORR) activity than conventional carbon-supported Pt catalysts [Kakinuma et al., 2011; Kakinuma et al., 2013; Senoo et al., 2014; Senoo et al., 2015; Shi et al., 2021]. These improvements are thought to arise from unique interfacial structures and from support-induced modifications of the electronic state of Pt nanoparticles. However, the fundamental relationship among interfacial charge transfer, local structural evolution, and catalytic behavior has not yet been fully clarified..

In this study, we focus on a Pt catalyst supported on Nb-doped SnO_2, which combines high electrical conductivity with excellent stability in acidic environments relevant to fuel-cell operation. To clarify how the support affects the Pt nanoparticles, we investigated a catalyst series in which performance improves with increasing Pt loading. Hard X-ray photoelectron spectroscopy (HAXPES) was used to probe interfacial structure and electronic state, X-ray absorption spectroscopy (XAS) was used to examine structural and electronic changes associated with catalyst–support interactions, and synchrotron infrared spectroscopy (Synchrotron IR) was employed to characterize the support surface. By combining these complementary techniques, we aim to clarify how electronic interactions between the ceramic support and Pt nanoparticles, as well as the resulting interfacial structures, contribute to the high activity of ceramic-supported Pt catalysts.

2. Methodology and Data

Nb-doped SnO_2 nanoparticles (Nb: 4 atomic %) prepared by the flame-spray method were used as the ceramic support, and Pt particles were deposited by a complex impregnation method, also known as the nanocapsule method. The obtained catalysts were heat-treated at 300 °C for 4 h under a nitrogen atmosphere containing 1% H_2. Three types of Nb-doped SnO_2-supported Pt catalysts (Pt/Nb-SnO_2) with Pt loadings adjusted to 15.9, 25.0, and 34.1 wt% were used. A carbon-supported Pt catalyst (TEC10E50E, Tanaka Kikinzoku Kogyo) was also employed as a reference sample.

The oxygen reduction activities of Pt/Nb-SnO_2 catalysts with Pt loadings similar to those used in this study (17.4, 26.2, and 34.2 wt%) have previously been reported and compared with those of the carbon-supported Pt catalyst. In that report, the activity of Pt/Nb-SnO_2 was comparable to or higher than that of the carbon-supported Pt catalyst and increased with increasing Pt loading. The 15.9 wt% Pt/Nb-SnO_2 catalyst showed activity comparable to that of the carbon-supported Pt catalyst, with both specific activity and mass activity being approximately 1.0 times those of the reference. For 25.0 wt% Pt/Nb-SnO_2, the specific activity and mass activity were 1.6 and 1.1 times higher, respectively, while for 34.1 wt% Pt/Nb-SnO_2, they were 2.1 and 1.5 times higher, respectively [Shi et al., 2021].

Before measurement, the samples were reduced under a hydrogen flow at room temperature to remove adsorbed oxygen. For the HAXPES measurements, the pretreated catalysts were introduced into the apparatus without exposure to air using an air-free transfer system. HAXPES measurements were performed at the SPring-8 industrial beamline SUNBEAM BL16XU. The incident X-ray energy was approximately 8 keV.

For the XAS measurements, the pretreated catalysts were placed in aluminum-laminated bags inside a glove box and sealed to prevent air exposure. XAS spectra at the Pt L_3-edge were collected at the SPring-8 industrial beamline SUNBEAM BL16B2. The X-ray beam was monochromatized using a Si(111) double-crystal monochromator, and higher-order harmonics were removed using a Rh-coated mirror at an incident angle of 3.5 mrad. The slit size before the sample was

adjusted to [value must be restored from the original experimental record]. The incident beam intensity was measured using a 17 cm ionization chamber filled with 100% N_2 gas.

Pt/Nb-SnO_2 was measured in fluorescence mode, and the fluorescence intensity was recorded using a 19-element semiconductor detector. The carbon-supported Pt catalyst was measured in transmission mode, and the transmitted beam intensity was measured using a 31 cm ionization chamber filled with 100% Ar gas. The resulting XAS spectra were analyzed using Athena. For synchrotron IR measurements, a very small amount of catalyst powder was thinly spread onto a BaF_2 window. The spectra were collected in transmission geometry under ambient temperature and atmospheric pressure, while flowing dry air to prevent moisture adsorption. Measurements were carried out at SPring-8 BL43IR using a permanently installed infrared microscope, Hyperion 2000, manufactured by Bruker. The spectral resolution was 4 cm^(-1), and the measurement area was approximately 10 μmin diameter.

In projects 2020A5390, 2021A5390, and 2021B5390, operando measurements of carbon-supported Pt nanoparticles had originally been planned. However, because ceramic-supported Pt catalysts suitable for elucidating the mechanisms responsible for high durability and high activity were successfully synthesized and evaluated, XAFS measurements of the ceramic-supported catalysts described in this report were conducted to address the original objectives from a more advanced perspective. Ultimately, the aim is to analyze reactions under high-temperature conditions through in situ measurements. However, to investigate the interfacial structure and related features in greater detail, structural analysis was first performed using ex situ XAS.
In project 2020A1706, which involved synchrotron IR measurements, analyzable spectra could not be obtained from the LPS-based all-solid-state battery electrodes that had initially been planned. Therefore, the measurements were instead carried out using the ceramic-supported catalysts described in this report. As a result, findings were obtained that contribute to the development of analytical methods for interfacial structures in electrochemical devices, which was the original objective of the study.

3. Results and Discussion

3.1 HAXPES analysis

Figure 1 shows the HAXPES results for the electronic states of the Pt, Nb, Sn, and O species in Pt/Nb-SnO_2. In the Pt $3d_{5/2}$ spectrum (Fig. 1a), the peak for the catalyst with a Pt loading of 15.9 wt% appears at a higher binding energy than that of metallic Pt. As the Pt loading increases, the peak shifts toward lower binding energy and approaches that of metallic Pt. This trend suggests that the extent of electron donation from Pt particles to the Nb-doped SnO_2 support becomes weaker at higher Pt loading, presumably because the interfacial electronic interaction per Pt atom is reduced as the Pt surface fraction increases.

In the Nb $2p_{3/2}$ spectrum (Fig. 1b), Nb remains stably in the pentavalent dopant state regardless of Pt loading, indicating that the Nb dopant state is not measurably altered by Pt deposition under the present conditions. In contrast, the Sn $3d_{5/2}$ and Sn $3d_{3/2}$ spectra show that the SnO_2 peak near 487 eV shifts toward lower binding energy with increasing Pt loading (Fig. 1c), suggesting an increase in electron density in the support region near the Pt/support interface.

A shoulder near 485.5 eV, assigned to PtSn alloy formation, is observed in the Sn 3d region, and its intensity increases with increasing Pt loading (Fig. 1c). This indicates that Pt–Sn interaction becomes more pronounced at higher Pt loading and supports the formation of an alloyed interfacial phase in addition to simple metal–support contact. Taken together, the HAXPES data directly demonstrate that Pt loading modifies the interfacial electronic structure and promotes PtSn-related features in Pt/Nb-SnO_2.

Previously reported conductivity measurements showed that the electronic conductivity increased by approximately two orders of magnitude when the Pt loading was increased from [insert value] to [insert value], consistent with relaxation of the electron-depletion layer formed by the Schottky barrier at the Pt/Nb-SnO_2 interface [Shi et al., 2021]. In that earlier study, electron donation from Pt and PtSn formation were proposed to facilitate charge transport across the interface. In the present work, the HAXPES results provide spectroscopic evidence that is consistent with that interpretation, although the conductivity itself was not remeasured here. Therefore, the present contribution is to clarify the interfacial electronic evolution by direct spectroscopic observation, while the conductivity enhancement and its quantitative magnitude should be attributed to the earlier report.

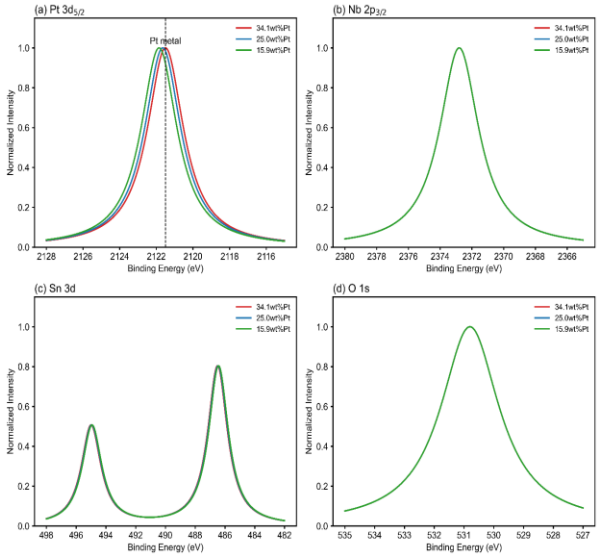

Figure 1. HAXPES spectra of (a) Pt $3d_{5/2}$, (b) Nb $2p_{3/2}$, (c) Sn 3d, and (d) O 1s for Pt/Nb-SnO_2 with Pt loadings of 15.9 wt%, 25.0 wt%, and 34.1 wt%.

3.2 XAS/EXAFS analysis

Next, the electronic state and local structure of the Pt nanoparticles were examined using Pt L_3-edge XAS for Pt/Nb-SnO_2. In the XANES spectra shown in Fig. 2a, Pt/Nb-SnO_2 and the carbon-supported Pt catalyst exhibit nearly identical spectral profiles, indicating that any electronic-state differences among the catalysts are too small to be clearly resolved by XAS under the present measurement conditions. This is consistent with the HAXPES results, which detected only subtle electronic changes.

Figure 2b shows the radial structure functions obtained by Fourier transformation of the EXAFS spectra. The peak in the 2–3 Å region, assigned mainly to Pt–Pt and Pt–Sn coordination, is lowest for TEC10E50E, whereas Pt/Nb-SnO_2 shows an increase in peak intensity with increasing Pt loading. This trend suggests that the average local coordination around Pt becomes larger as the Pt loading increases.

Consistent with this interpretation, the average particle size of the Pt nanoparticles in TEC10E50E is 2.5 nm, whereas the average particle sizes of Pt/Nb-SnO_2 are approximately 2.5–3.0 nm for 15.9 wt%, 3.0–3.5 nm for 25.0 wt%, and around 3.5 nm for 34.1 wt%. This indicates particle growth with increasing Pt loading, which reduces the relative fraction of low-coordination surface atoms and therefore increases the average coordination number.

In addition, the high-intensity peak corresponding to Pt–Pt coordination shifts toward longer radial distances for Pt/Nb-SnO_2 compared with TEC10E50E as the Pt loading increases. This result indicates a change in the Pt local structure with loading. Together with the HAXPES results, these EXAFS observations are consistent with interfacial electronic interaction and possible Pt–Sn alloy-related structural modification, but they do not by themselves prove the catalytic origin of the activity enhancement. Therefore, the structural changes should be presented as supporting evidence rather than as direct proof of the active site.

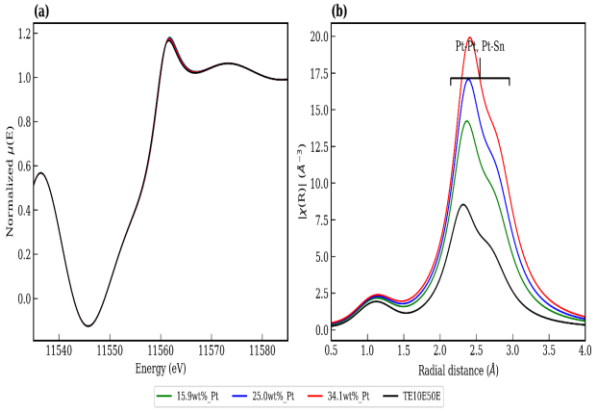

Figure 2. (a) Pt L_3-edge XANES spectra and (b) radial structure functions obtained by Fourier transformation of the EXAFS spectra for Pt/Nb-SnO_2 with Pt loadings of 15.9 wt%, 25.0 wt%, and 34.1 wt%, and for the carbon-supported Pt catalyst (TEC10E50E).

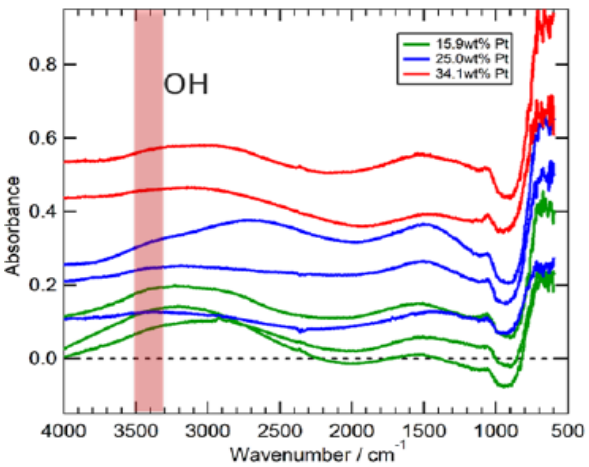

Figure 3. Synchrotron IR spectra of Pt/Nb-SnO_2 with Pt loadings of 15.9 wt%, 25.0 wt%, and 34.1 wt%.

3.3 Synchrotron IR analysis

Finally, synchrotron IR spectroscopy was used to examine whether surface functional groups on Pt/Nb-SnO_2 vary with Pt loading and may contribute to catalyst surface modification. It has been reported that surface functional groups on the support can influence local mass transport, modify metal–support interactions, and affect the electronic state of supported Pt nanoparticles, potentially contributing to catalytic activity [Andrews et al., 2015; Schwab, 1970; Tauster et al., 1978; Horsley, 1979; Dulub et al., 2000].

Although oxygen-containing surface species can sometimes be examined by photoelectron spectroscopy, such signals are obscured by the SnO_2 support signal in the present system, as shown in Fig. 1(d). Therefore, synchrotron IR was selected because it can distinguish functional-group vibrations from the support background and is sufficiently sensitive for measurements on individual catalyst particles dispersed on a BaF_2 window. Figure 3 presents multiple measurements of individual Pt/Nb-SnO_2 particles with Pt loadings of 15.9 wt%, 25.0 wt%, and 34.1 wt%, dispersed thinly on a BaF_2 window. In the region around 3400 cm^{-1}, which is often associated with hydroxyl groups in carbon-supported catalysts, no clearly discernible hydroxyl-band signal was observed for the Nb-SnO_2-supported samples.

However, the spectral features were broad, and it is possible that weak signals were not fully resolved under the present measurement conditions. Therefore, the present data do not allow a definitive conclusion that hydroxyl groups are absent; rather, they indicate that any such signal, if present, is below the current detection level or is masked by the broad background. In addition, no systematic dependence on Pt loading was observed within the present data set. Thus, any effect of surface functional groups on catalytic performance remains tentative and should be verified by more sensitive quantitative and spatially resolved IR measurements in future work.

4. Conclusion

Regarding ceramic-supported Pt catalysts, we investigated the interfacial interactions and the factors contributing to the catalytic properties by analyzing the interfacial electronic state, local structure of Pt nanoparticles, and the support surface using HAXPES, XAS/EXAFS, and synchrotron IR for SnO_2-supported Pt catalysts.

From HAXPES, we obtained direct spectroscopic evidence of electron donation from Pt nanoparticles to the SnO_2 support and the formation of a PtSn alloy at the interface. These electronic modifications were found to be more pronounced as Pt loading increased. Complementary XAS/EXAFS analysis indicated corresponding changes in the local coordination environment of Pt. These combined spectroscopic findings are consistent with the relaxation of the electron-depletion layer at the interface, which is thought to facilitate charge transport and contribute to the catalytic performance observed in previous electrochemical studies.

In the synchrotron IR analysis, hydroxyl and other surface functional groups were not clearly resolved for Pt/Nb-SnO_2 under the current measurement conditions. While this suggests that the direct influence of such groups on activity might be relatively small compared to interfacial electronic effects, the broad spectral features indicate that potential weak signals might remain undetected. Therefore, future work utilizing advanced quantification and high-resolution spatial distribution methods is necessary to definitively clarify the role of support surface functional groups in metal–support interactions. For next-generation fuel cells, developing catalysts that exhibit stable performance and durability at high temperatures remains a priority, and ceramic-supported Pt-based catalysts are a promising pathway. We expect that applying the integrated spectroscopic methodology established here to newly developed systems will provide critical design guidelines for high-performance ceramic-supported electrocatalysts.

Acknowledgments

The authors would like to express their sincere gratitude to the Editor-in-Chief for their guidance and support throughout the review process. We are also deeply indebted to the two anonymous reviewers for their insightful comments, constructive feedback, and valuable suggestions, which significantly improved the quality and clarity of this manuscript.

Declarations

Data and code availability

All data generated or analyzed during this study are available from the corresponding author upon reasonable request. No computational code was used in this study.

Conflicts of interest

The authors announced that they have no known conflicts of interest or personal relationships that could have appeared to influence the work reported in this manuscript.

Ethical approval

The authors declare no ethical issues; the research was carried out in full agreement with ethical standards. Also, this paper is neither under Review nor published elsewhere.

References

Andrews, S. P., Stepan, A. F., Tanaka, H., Ley, S. V., & Smith, M. D. (2005). Heterogeneous or homogeneous? A case study involving palladium-containing perovskites in the Suzuki reaction. Advanced Synthesis & Catalysis, 347(5), 647-654.

Dulub, O., Hebenstreit, W., & Diebold, U. (2000). Imaging cluster surfaces with atomic resolution: The strong metal-support interaction state of Pt supported on TiO_2 (110). Physical Review Letters, 84(13), 3646-3649.

Fabbri, E., Pătru, A., Rabis, A., Kötz, R., & Schmidt, T. J. (2014a). Advanced cathode materials for polymer electrolyte fuel cells based on Pt/ metal oxides: From model electrodes to catalyst systems. Chimia, 68(4), 217-222. https://doi.org/10.2533/chimia.2014.217

Fabbri, E., Rabis, A., Kötz, R., & Schmidt, T. J. (2014b). Pt nanoparticles supported on Sb-doped SnO_2 porous structures: developments and issues. Physical Chemistry Chemical Physics, 27. https://doi.org/10.1039/C4CP00238E

Goto, K. (2022, August 8). NEDO ni okeru nenryō denchi suiso kanren jigyō no torikumi [Efforts in Fuel Cell and Hydrogen Related Business at NEDO]. FC-Cubic Open Symposium Homepage. http://fc-cubic-event.jp/wp-sympo/wp-content/uploads/2020/10/seisaku.pdf

Horsley, J. A. (1979). A molecular orbital study of strong metal-support interaction between platinum and titanium dioxide. Journal of the American Chemical Society, 101(11), 2870-2874. https://doi.org/10.1021/ja00505a011

Kakinuma, K., Chino, Y., Senoo, Y., Uchida, M., Kamino, T., Uchida, H., Deki, S., & Watanabe, M. (2013). Characterization of Pt catalysts on Nb-doped and Sb-doped SnO_2 support materials with aggregated structure by rotating disk electrode and fuel cell measurements. Electrochimica Acta, 110, 316-324. https://doi.org/10.1016/j.electacta.2013.06.127

Kakinuma, K., Uchida, M., Kamino, T., Uchida, H., & Watanabe, M. (2011). Synthesis and electrochemical characterization of Pt catalyst supported on $Sn_{0.96}Sb_{0.04}O_2$-δ with a network structure. Electrochimica Acta, 56(7), 2881-2887. https://doi.org/10.1016/j.electacta.2010.12.077

Ozouf, G., Cognard, G., Maillard, F., Chatenet, M., Guétaz, L., Heitzmann, M., Jacques, P. A., & Beauger, C. (2018). Sb-Doped SnO_2 aerogels based catalysts for proton exchange membrane fuel cells: Pt deposition routes, electrocatalytic activity and durability. Journal of The Electrochemical Society, 165(6), F3036. https://doi.org/10.1149/2.0041806jes

Schwab, G.-M. (1970). Chemical effects at the solid/solid phase boundary. Journal of Colloid and Interface Science, 34(3), 337-342.

Senoo, Y., Kakinuma, K., Uchida, M., Uchida, H., Deki, S., & Watanabe, M. (2014). Improvements in electrical and electrochemical properties of Nb-doped SnO_2-δ supports for fuel cell cathodes due to aggregation and Pt loading. RSC Advances, 4, 17353-17361. https://doi.org/10.1039/C4RA03988B

Senoo, Y., Taniguchi, K., Kakinuma, K., Uchida, M., Uchida, H., Deki, S., & Watanabe, M. (2015). Cathodic performance and high potential durability of Ta-SnO_2-δ-supported Pt catalysts for PEFC cathodes. Electrochemistry Communications, 51, 37-40. https://doi.org/10.1016/j.elecom.2014.12.005

Shi, G., Tano, T., Tryk, D. A., Iiyama, A., Uchida, M., & Kakinuma, K. (2021). Temperature Dependence of Oxygen Reduction Activity at Pt/Nb-SnO_2 Catalysts with Varied Pt Loading. ACS Catalysis, 11(9), 5222-5230. https://doi.org/10.1021/acscatal.0c05157

Tauster, S. J., Fung, S. C., & Garten, R. L. (1978). Strong metal-support interactions. Group 8 noble metals supported on titanium dioxide. Journal of the American Chemical Society, 100(1), 170-175. https://doi.org/10.1021/ja00469a029

Yin, M., Xu, J., Li, Q., Jensen, J. O., Huang, Y., Cleemann, L. N., Bjerrum, N. J., & Xing, W. (2014). Highly active and stable Pt electrocatalysts promoted by antimony-doped SnO_2 supports for oxygen reduction reactions. Applied Catalysis B: Environmental, 144, 112-120. https://doi.org/10.1016/j.apcatb.2013.07.007